Identification of a chemical fingerprint linking the undeclared 2017 release of ^{106}Ru to advanced nuclear fuel reprocessing

Michael W. Cooke[a,1], Adrian Botti[a], Dorian Zok[b], Georg Steinhauser[b], and Kurt R. Ungar[a]

[a]Radiation Protection Bureau, Health Canada, Ottawa, ON K1A 1C1, Canada; and [b]Institute of Radioecology and Radiation Protection, Leibniz Universität Hannover, 30419 Hannover, Germany

The undeclared release and subsequent detection of ruthenium-106 (^{106}Ru) across Europe from late September to early October of 2017 prompted an international effort to ascertain the circumstances of the event. While dispersion modeling, corroborated by ground deposition measurements, has narrowed possible locations of origin, there has been a lack of direct empirical evidence to address the nature of the release. This is due to the absence of radiological and chemical signatures in the sample matrices, considering that such signatures encode the history and circumstances of the radioactive contaminant. In limiting cases such as this, we herein introduce the use of selected chemical transformations to elucidate the chemical nature of a radioactive contaminant as part of a nuclear forensic investigation. Using established ruthenium polypyridyl chemistry, we have shown that a small percentage (1.2 ± 0.4%) of the radioactive ^{106}Ru contaminant exists in a polychlorinated Ru(III) form, partly or entirely as β-^{106}RuCl$_3$, while 20% is both insoluble and chemically inert, consistent with the occurrence of RuO$_2$, the thermodynamic endpoint of the volatile RuO$_4$. Together, these findings present a clear signature for nuclear fuel reprocessing activity, specifically the reductive trapping of the volatile and highly reactive RuO$_4$, as the origin of the release. Considering that the previously established ^{103}Ru:^{106}Ru ratio indicates that the spent fuel was unusually young with respect to typical reprocessing protocol, it is likely that this exothermic trapping process proved to be a tipping point for an already turbulent mixture, leading to an abrupt and uncontrolled release.

ruthenium | polypyridyl complex | radiochemistry | nuclear forensics

In the fall of 2017, the man-made, high-yield fission product ^{106}Ru (half-life, $t_{1/2}$ = 373.6 d) was detected by monitoring networks across Europe (1–4), along with sporadic detections of minute amounts of the relatively short-lived ^{103}Ru ($t_{1/2}$ = 39.2 d) in select locations. Although unprecedented in scale (250 TBq) (5), airborne and surface measurements substantiated a timely assessment that there was no detrimental impact to human health (6). Nevertheless, the undeclared intrusion of such radioactivity into the air space and soil of sovereign nations demands investigation, in support of national and coordinated global security.

To address the location of the ^{106}Ru source, recent reports have used dispersion modeling and field measurements of ^{106}Ru concentration (airborne and ground deposition) to demonstrate an origin in the Southern Urals of Russia, in the area of the Mayak industrial complex (1, 5–9). A long history of nuclear-related activities in this area, combined with the radiopurity of the field observations and the detection of the short-lived ^{103}Ru, lends credence to the scenario of an accidental release during nuclear fuel reprocessing and serves to dispel some persistent theories on the origin of the release (e.g., nuclear reactor accident, downed radioisotope thermoelectric generator satellite, volatilized medical sources, etc.) (1). However, to make a direct link to fuel reprocessing activity on this basis alone is circumstantial and as such provides room for plausible deniability. Direct evidence to this end

constitutes the identification of unique signatures. From a radiological perspective, there is none. Samples have been shown to be radiopure and to carry the stable ruthenium isotopic signature of civilian spent nuclear fuel (10), while stable elemental analysis by scanning electron microscopy and neutron activation has revealed no detectable anomalies compared to aerosol filter media sampled prior to the advent of the ^{106}Ru contaminant (1, 11). We are, then, left with the definition of a limiting case for a nuclear forensic investigation.

Fortunately, we are concerned with an element that has significant covalent character to its bonding interactions (12). This affords the opportunity to perform chemical transformations, with and without the presence of a stable form of the same element. By selecting reactions that are well understood and/or by varying reaction conditions, we can compare the distribution of the radioactive element to the stable form in the reaction product(s) (Scheme 1). In this way, it is possible to deduce both general and highly specific information about the atomic connectivity, that is, the chemical context, of the radioactive contaminant, given that the rules for reactivity are well understood.

Results and Discussion

To help refine synthetic targets amenable to the strategy proposed in Scheme 1, we subscribe to the hypothesis that the

Significance

In the fall of 2017, a massive, undeclared release of ^{106}Ru occurred that was detected across Eurasia. To conclusively address the nature of the release, we have used carefully selected and established chemical transformations to reveal a chemical fingerprint for the ^{106}Ru contaminant that is uniquely consistent with specific methodology employed in the reprocessing of spent nuclear fuel. In view of international attention and investigation to date, this chemical fingerprint is the first direct evidence to this effect. This work serves, by example, as a potentially valuable addition to the field of nuclear forensics, considering that it is the only means to extract historical information from a radiopure contaminant in the absence of stable elemental anomalies.

CHEMISTRY

Scheme 1. High-level concept depicting the reactive incorporation of both stable (green) and radioactive (red) chemical species of an element into isostructural end products.

release of ^{106}Ru into the environment is associated with fuel reprocessing activity. Owing to its complex chemistry and high specific activity (typically 6 to 9% of fission products) in spent nuclear fuel (12–16), the removal of radio-ruthenium from waste streams poses a significant challenge. While a myriad of approaches has been proposed, the vast majority center about the PUREX (plutonium–uranium extraction) process where the recovery of uranium and plutonium is accomplished by liquid extraction with an organophosphate from fuel that is digested in nitric acid (16–18). To amplify the oxidative power of the mixture, oxidants such as ceric ammonium nitrate can be added to encourage the evolution of the volatile and highly reactive RuO_4, which can then be driven off with carrier gas and subsequently trapped or passivated. At this early dissolution stage, and later during the vitrification of raffinates, the condensation and decomposition of RuO_4 to relatively inert oxides inside the containment vessels can lead to problems of accumulated dose and accelerated corrosion (14, 15, 19, 20). To address this, considerable investigative effort has been made to remove ruthenium at the fuel dissolution phase (17, 21, 22). Nevertheless, the formation of RuO_4 is still a very appealing option with respect to simplicity, cost, and scalability, as evidenced by recent investigations into ruthenium volatilization through RuO_4 generation (23–26). Subsequent chemical reduction of RuO_4 to more passive forms is also appealing with respect to such considerations, despite introducing additional waste material for management. Some of the more notable options in this regard are the efficient formation of RuO_4^{-2} and RuO_4^{-} salts under alkaline conditions (21, 27), the formation of RuO_2 on contact with reducing media (26, 28), and the generation of Ru(III) and Ru(IV) polychlorinated complexes in hydrochloric acid (29–31).

Treatment of filter pieces from both German and Swedish radionuclide surveillance networks with solvent gave highly reproducible results for partitioning of the ^{106}Ru contaminant. Good partitioning reproducibility, in conjunction with autoradiographic imaging (*SI Appendix*, Fig. S21), supports a homogenously distributed contaminant. We have found that $51.3 \pm 2.4\%$ of the ^{106}Ru contaminant was associated with the aqueous extract. This result is in very good agreement with that determined by other laboratories (1) and clearly indicates that the ^{106}Ru is composed of more than one chemical form. Partitioning experiments similarly performed with carbon tetrachloride showed no discernable association with the ^{106}Ru contaminant. This indicates an absence of adsorbed RuO_4, which is typically soluble in carbon tetrachloride, one of the few solvents that does not succumb to attack by this powerful oxidizing agent (13). This is not surprising, since RuO_4 decomposes to RuO_2 (hydrated) in water under ambient conditions and further upon exposure to light (15, 32), while reoxidation of RuO_2 back to RuO_4 is very slight and reserved for atmospheric oxidants such as ozone (32). Interestingly, we found that a small but highly reproducible fraction ($7.35 \pm 0.70\%$) of the ^{106}Ru contaminant was partitioned into ethanol. This result further supports a multicomponent composition for the ^{106}Ru contaminant. In light of the aforementioned discussion regarding the pragmatic treatment of RuO_4 in nuclear fuel reprocessing, β-$RuCl_3$ is expected to be formed from the passivation of RuO_4 in HCl to an extent that depends directly upon time and temperature

(30, 31). Among inorganic ruthenium compositions, it is noteworthy that β-$RuCl_3$ possesses the rare quality of being highly soluble in dative solvents. Thus, we have chosen to explore the hypothesis that the passivation of RuO_4 in HCl was implicated in the environmental release.

This hypothesis informs an appropriate selection of chemical reactions and synthetic targets toward revealing a unique signature, and other meaningful chemical information, about the ^{106}Ru contaminant. To this end, polypyridyl chemistry is appealing as a reactive vehicle to incorporate ^{106}Ru, since such ruthenium complexes are exceptionally robust and formed in high yield under ambient conditions. Also, characteristic charge-transfer electronic transitions that lie in the visible region of the spectrum make these complexes intensely colored, facilitating chromatographic separation (33, 34). Of the polypyridyl ligands available, those derived from the tridentate 2,2′:6′,2″-terpyridine ligand are particularly well-suited as they offer achiral products and superior kinetic stability (33). Considering the ease of synthesis afforded by one-pot procedures to form 4′-substituted analogs of 2,2′:6′,2″-terpyridine, we have elected to synthesize 4′-p-tolyl-2,2′:6′,2″-terpyridine (ttpy; Fig. 1) according to reported procedures (35, 36), albeit with a notable exception regarding its purification (*Materials and Methods*). With this ligand in hand, we are supported by a plethora of established ruthenium coordination chemistry, the vast majority of which is derived from reaction with β-$RuCl_3$. In particular, we have identified the subsequent monoligated complex, ttpyRuCl$_3$ (37), and the reduced, bis-ligated complex, Ru(ttpy)$_2$$^{2+}$ (38), as targeted reaction products for isolation and radiometric measurement, in adherence to the general strategy presented in Scheme 1. Although the former has invariably served as a reaction intermediate to the formation of heteroleptic complexes (39, 40), it takes center stage in this work. This is due to the fact that the formation of ttpyRuCl$_3$ (or related complexes based upon 2,2′:6′,2″-terpyridine) is expected to be highly selective to β-$RuCl_3$ and related compounds, considering that there is no alteration in oxidation state or local coordination geometry about the ruthenium atom. In fact, to the best of our knowledge, the formation of ttpyRuCl$_3$ has only ever been performed from β-$RuCl_3$. Therefore, by investigating the formation of ttpy^{106}RuCl$_3$ from the relatively small proportion of the ^{106}Ru contaminant that is extractable in ethanol and by demonstrating the highly selective nature of the reaction, we can speak to the existence of β-^{106}RuCl$_3$. In this way, we may determine whether or not passivation of RuO_4 in hydrochloric acid was invoked.

Radiochemistry 1: Synthesis and Purification of ttpyRuCl$_3$ in the Presence of ^{106}Ru. With the tridentate ligand (ttpy) in hand, reaction of 1.1 equivalents with β-$RuCl_3$ proceeds in high yield (>80%) from ethanolic solution, provided that the reactant concentration is >0.01 M. The overall radiochemical reaction is presented in Scheme 2 (see also *SI Appendix*, Fig. S16), and experimental details are provided in *Materials and Methods*. Ethanol containing leached ^{106}Ru (74.5 ± 5.3 mBq ^{106}Ru) was used to synthesize ttpyRuCl$_3$ from stable β-$RuCl_3$ in 88% yield (0.12 g theoretical yield). The insoluble precipitate formed was isolated and counted using a high-purity germanium well detector, using the gamma photon emission at 622 keV (9.93% intensity) associated with the short-lived ^{106}Rh progeny as the analytical signal. Relative to the ethanol extract, $28.8 \pm 3.5\%$ of the ^{106}Ru activity was found to be localized in the initial precipitated material. The remaining ethanolic filtrate was chromatographed on silica gel using an eluent mixture of acetonitrile and saturated, aqueous potassium nitrate solution (7:1, respectively) to isolate the sole by-product, Ru(ttpy)$_2$$^{2+}$, after work-up with NH$_4PF_6$. This material was similarly gamma-counted and was found to contain $11.2 \pm 2.0\%$ (8.37 ± 1.41 mBq) of the ^{106}Ru activity from the ethanol extract. In contrast to the fate of the stable ruthenium, this is a sizeable proportion of ^{106}Ru. However,
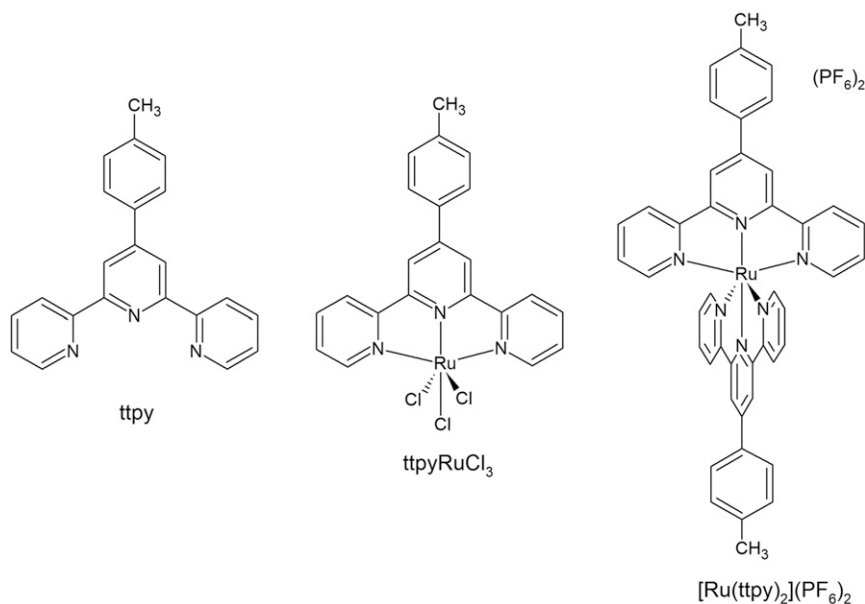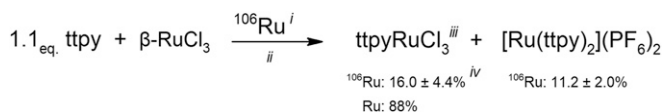
Fig. 1. Synthetic targets used to evaluate the reactivity and distribution of ^{106}Ru.

this is quite reasonable considering that the 0.1 equivalent excess of ttpy used in the reaction (i.e., 7.5 mg) constitutes an enormous molar excess over ^{106}Ru (4.03×10^{12}-fold), and that inorganic ruthenium species other than β-RuCl$_3$ will react to form Ru(ttpy)$_2^{2+}$ under these conditions. Again, we see evidence of a complex, multicomponent ^{106}Ru contaminant.

While $28.8 \pm 3.5\%$ of the ethanol-extracted ^{106}Ru was found to be isolated with the stable product, ttpyRuCl$_3$, consideration of potential flocculation effects precluded the conclusion that ttpy^{106}RuCl$_3$ was formed to any extent. To address this, a high-performance liquid chromatography (HPLC) method was developed to separate ttpyRuCl$_3$ from Ru(ttpy)$_2^{2+}$, and from other environmental contaminants associated with the filter material. This HPLC method was first developed on an analytical scale and later adapted to a semi-preparative one, using a C$_{18}$ stationary phase and a mobile phase consisting of an isocratic mixture of N,N'-dimethylformamide (DMF) and methanol (90:10, respectively), optimized at 1.30 mM of tetrabutylammonium chloride (*SI Appendix*, Figs. S14 and S15). Note that method development was confined by the limited solubility of ttpyRuCl$_3$ (appreciably soluble in N,N'-DMF, tolerating no more than 30% methanol) and that effective separation of ttpyRuCl$_3$ and Ru(ttpy)$_2^{2+}$ was afforded mainly by the addition of the tetrabutylammonium chloride. The characteristic ligand-to-metal and metal-to-ligand charge-transfer bands that characterize ttpyRuCl$_3$ and Ru(ttpy)$_2^{2+}$, respectively, were used to arrive at a detection wavelength of 450 nm in the electronic spectrum.

The entirety of the crude ttpyRuCl$_3$ isolated in Scheme 2 (108 mg, 20.9 ± 2.5 mBq ^{106}Ru) was purified by HPLC (Fig. 2). Fractions collected at set times in the HPLC purification process were combined and concentrated for gamma counting. The very small amount of ^{106}Ru measured in these reaction components required long detection count times ranging from 1 to 2 Ms. For

this range of count time, the concomitant span of detection capabilities, as defined by the critical limit (L$_c$) and detection limit (L$_d$) at 95% confidence, corresponded to L$_c$ = 3.7 mBq and L$_d$ = 7.5 mBq for 1 Ms and L$_c$ = 2.9 mBq and L$_d$ = 5.9 mBq for 2 Ms. Nevertheless, a very good account of the initial ^{106}Ru in the crude ttpyRuCl$_3$ was provided by the components of the HPLC purification process. The elution peak at retention time (R$_t$) = 2.96 min, corresponding to ttpyRuCl$_3$, was found to contain 10.2 ± 2.6 mBq of ^{106}Ru (Fig. 3), while the fraction collected from 0 to 2.0 min, representing unretained material from the column hold-up volume, was found to contain 12.7 ± 3.1 mBq of ^{106}Ru (*SI Appendix*, Figs. S19 and S20). These quantities represent $48.7 \pm 13.2\%$ (ttpyRuCl$_3$) and $60.9 \pm 14.8\%$ (unretained) of the
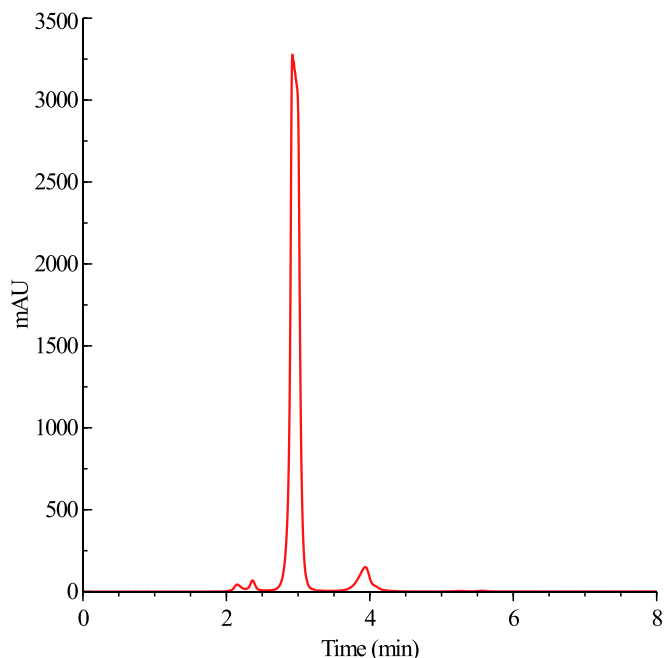
Fig. 2. HPLC purification of ttpyRuCl$_3$ (R$_t$ = 2.96 min) that precipitated from the radiochemical reaction described in Scheme 2. Monitored at λ = 450 nm.

$1.1_{eq.}$ ttpy + β-RuCl$_3$ $\xrightarrow[\text{ii}]{^{106}\text{Ru}^{\,i}}$ ttpyRuCl$_3^{\,iii}$ + [Ru(ttpy)$_2$](PF$_6$)$_2$

^{106}Ru: 16.0 ± 4.4% ^{iv} ^{106}Ru: 11.2 ± 2.0%
Ru: 88%

Scheme 2. Reaction targeting the formation of ttpyRuCl$_3$ in the presence of ^{106}Ru. ^{i}^{106}Ru obtained from ethanol extraction. ^{ii}Two hours at reflux temperature. ^{iii}Purified by reverse-phase HPLC. ^{iv}Adjusted for chemical recovery.

^{106}Ru measured in the crude ttpyRuCl$_3$ before purification. The unretained fraction of ^{106}Ru likely consists of unreactive species removed by flocculation as ttpyRuCl$_3$ precipitated from the reaction solution.

Radiochemistry 2: Reaction of ^{106}Ru without Stable Ru Precursor. To provide additional insight and validation, particularly in light of the relatively large counting uncertainty associated with the gamma measurements of the preceding radiochemical experiment (Scheme 2), an analogous experiment was performed without the use of stable ruthenium precursor. In this instance, the formation of the reduced, bis-ligated complex [^{106}Ru(ttpy)$_2$]$^{2+}$ was targeted (Scheme 3 and *SI Appendix*, Fig. S18). The reaction to form [Ru(ttpy)$_2$]$^{2+}$ from 2.1 equivalents of ttpy in ethanol alone was found to be more broadly applicable than previously believed, proceeding smoothly from both Ru(III) and Ru(IV) precursors containing suitable counter anions, as demonstrated by chemical recoveries obtained with β-RuCl$_3$ (89%), (NH$_4$)$_2$RuCl$_6$ (94%), and Ru(NO)(NO$_3$)$_3$ (90%). Thus, we can use an excess of ttpy to compare the reactive fractions of the ^{106}Ru contaminant (extractable in ethanol) obtained from both carrier and carrier-free approaches (Table 1).

Here, a mere 0.20 mg of ttpy amounted to an extraordinary molar excess (1.7×10^{10}-fold) relative to ^{106}Ru. Following termination of the reaction, stable [Ru(ttpy)$_2$](PF$_6$)$_2$ was added as a tracer to enable chromatographic purification. Gamma counting of the isolated fraction revealed that $28.6 \pm 2.6\%$ (0.137 ± 0.013 Bq) of the ^{106}Ru from the ethanol extract was colocated with the added [Ru(ttpy)$_2$](PF$_6$)$_2$. A spectral overlay of the gamma-counted reaction components is presented in Fig. 3. From Table 1, summing contributions of the isolated components from the β-RuCl$_3$ radiochemical reaction (Scheme 2, ttpyRuCl$_3$ and Ru(ttpy)$_2^{2+}$), we find a total reactive fraction of $27.2 \pm 9.0\%$. This result is in excellent agreement with the reactive fraction found for the corresponding carrier-free reaction (Scheme 3). Such an intersection of results strengthens further the identification and contribution of ttpy^{106}RuCl$_3$ and additionally serves

$$\text{ttpy}_{(excess)} + {}^{106}\text{Ru}^{\textit{i}} \xrightarrow[\textit{iii}]{[\text{Ru(ttpy)}_2](\text{PF}_6)_2{}^{\textit{ii}}} [{}^{106}\text{Ru(ttpy)}_2](\text{PF}_6)_2$$

^{106}Ru: 28.6 ± 2.6%
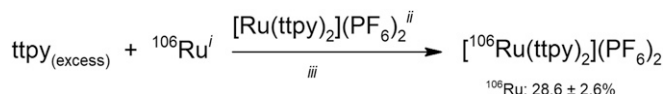
Scheme 3. Reaction to form [^{106}Ru(ttpy)$_2$](PF$_6$)$_2$. $^{i\,106}$Ru obtained from ethanol extraction. ^{ii}Stable complex added postreaction as a tracer for chromatographic isolation. ^{iii}Ethanol, 90 °C, 16 h.

to provide a more accurate uncertainty estimate considering the higher activity (i.e., lower counting uncertainty) afforded by the carrier-free reaction (Fig. 3).

Formation of ttpyRuCl$_3$: Reaction Selectivity. While the formation of ttpyRuCl$_3$ has only ever been performed from β-RuCl$_3$ (37, 40), we undoubtedly expect the reaction to proceed to an appreciable extent from higher-order polychlorinated Ru(III) compounds, given the favorable binding interaction afforded by the tridentate ligand, ttpy, and considering that their solution equilibria in dative solvent will include the formation of RuCl$_3$ (41, 42). Nevertheless, by defining the applicable scope of this reaction, we refine and gain confidence in the types of contaminant ruthenium species that could lead to the observed formation of ttpy^{106}RuCl$_3$. Instead of testing an exhaustive selection, several compounds were chosen that reflect a systematic variation from soluble polychlorinated Ru(III) species, namely, variation with respect to ruthenium valency, exchangeable supporting ligands, and physical format. To this end, we had selected the polychlorinated Ru(IV) salt, (NH$_4$)$_2$RuCl$_6$, the Ru(III) mixture, Ru(NO)(NO$_3$)$_3$ (in nitric acid), and the highly insoluble allotrope to β-RuCl$_3$, α-RuCl$_3$. In nitric acid solution, what is denoted commercially as Ru(NO)(NO$_3$)$_3$ is actually a mixture of ruthenium (III/IV) complexes varying in proportion of coordinated and exchangeable nitrate, nitrite, and water molecules, depending on solution conditions (16, 43); moreover, it is directly representative of the nitric acid-based oxidative mixtures
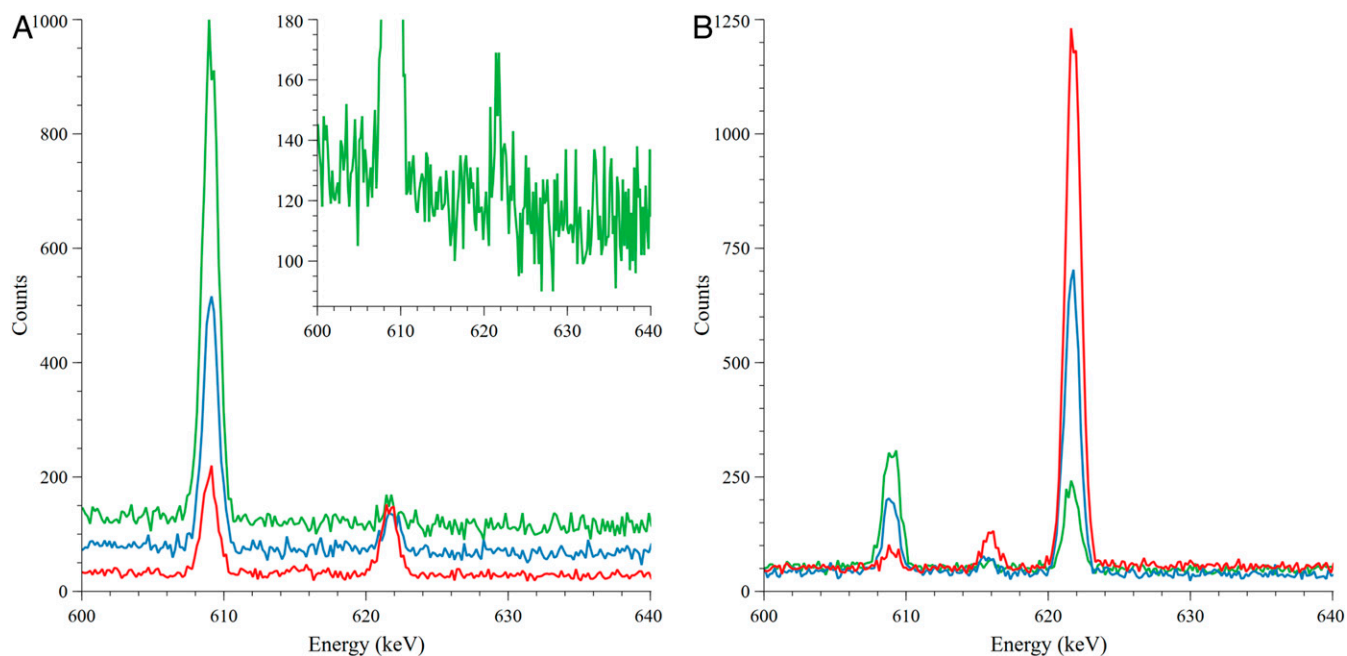
Fig. 3. Overlay of gamma spectra, in the analytical region of interest (600 to 640 keV) for ^{106}Ru measured in the reaction components leading to the formation and isolation of ttpyRuCl$_3$ (*A*) and [^{106}Ru(ttpy)$_2$](PF$_6$)$_2$ (*B*). Depicted are gamma emission peaks corresponding to ^{214}Bi (609 keV, naturally occurring) and ^{106}Ru (616 and 622 keV). (*A*) Ethanol extract (red); crude ttpyRuCl$_3$ (blue); purified ttpyRuCl$_3$ (green). (*B*) Filter piece (red); ethanol extract (blue); isolated fraction colocated with added [Ru(ttpy)$_2$](PF$_6$)$_2$ (green).

Table 1. Allocation of ^{106}Ru in the radiochemical reactions relative to the initial quantity measured in the ethanol extract

Reaction	ttpyRuCl$_3$ (% ^{106}Ru, k = 1)	[Ru(ttpy)$_2$](PF$_6$)$_2$ (% ^{106}Ru, k = 1)	Reactive fraction of ^{106}Ru, %
ttpy + β-RuCl$_3$ + ^{106}Ru	14.0 ± 3.9* (16.0 ± 4.4)[†]	11.2 ± 2.0	27.2 ± 9.0
ttpy + ^{106}Ru	—	28.6 ± 2.6	28.6 ± 2.6

*Isolated ttpyRuCl$_3$ fraction from HPLC (R$_t$ = 2.96 min).
[†]Adjusted for chemical recovery.

used to dissolve spent fuel early in the PUREX process (16, 17). Subjecting these model compounds to the reaction conditions used to synthesize ttpyRuCl$_3$ (*Materials and Methods*), with the notable exception of using saturated ethanolic and aqueous ethanolic solutions of potassium chloride in the case of Ru(NO)(NO$_3$)$_3$, produced no discernable trace of ttpyRuCl$_3$ (Table 2). These tests demonstrate that the reactive tolerance is limited to polychlorinated ruthenium (III) compositions. Therefore, we can conclude that the isolated ttpy^{106}RuCl$_3$ in these experiments originated from ^{106}Ru filter contaminant that exists as β-^{106}RuCl$_3$ or, more generally, [^{106}RuCl$_n$(H$_2$O)$_{6-n}$]$^{3-n}$. Considering the sequential fractionation of ^{106}Ru in the described experiments, from filter material to ethanolic extract (7.35 ± 0.70%) to precipitated ttpyRuCl$_3$ (28.8 ± 3.5% with 88% chemical recovery) to HPLC isolated ttpyRuCl$_3$ (48.7 ± 13.2%), we determine that 1.17 ± 0.36% of the filter contaminant exists in this chemical form.

Assessment of the Bulk ^{106}Ru Contaminant. That a small proportion of the ^{106}Ru contaminant is composed of polychlorinated ^{106}Ru(III) species is direct evidence that fuel reprocessing was the origin of the 2017 environmental release. Plausible reprocessing activities that could lead to such compounds are limited to either the reductive trapping of oxidatively generated RuO$_4$ in hydrochloric acid (29–31) or the electrochemical reduction and metallization of uranium in spent fuel from molten alkali chloride mixtures (44–46). Fortunately, the compositions formed from both approaches differ substantially. An interrupted process involving the reductive trapping of RuO$_4$ in hydrochloric acid would reasonably be expected to contain some measure of the inert RuO$_2$, owing to the decomposition of RuO$_4$, along with a mixture of Ru(IV) and Ru(III) chloro complexes, the proportion of which will depend upon temperature, duration, and HCl concentration but should favor heavily the reduction to Ru(IV) (30, 31). Mixed nitrosyl–nitrate–nitrite Ru(III/IV) complexes derived from an oxidative nitric acid slurry used to generate the RuO$_4$ may also become entrained upon release, depending on the system engineered. In the case of the pyroprocessing of spent fuel from molten alkali chloride mixtures, chloro complexes are exclusively formed and, although dependent on melt temperature and duration, center upon the formation of Ru(III) chloro complexes with some disproportionation/decomposition to metallic ruthenium occurring very slowly at temperatures >550 °C (44).

By investigating the reactive nature of the bulk of the ^{106}Ru contaminant, we may reveal additional information to help discern between these scenarios. To do this, we have selected commercially available ruthenium compounds representative of the types encountered in such reprocessing activities (Table 2). These compounds comprise a diverse array, differentiated by ruthenium valency, supporting ligand, and physical format, and we can use them to characterize an appropriate reaction (i.e., establish the rules of reactivity). Then, by applying the reactive conditions to the ^{106}Ru contaminant and tracking its subsequent fate and distribution, we may make reasonable deductions about the bulk chemical composition of the ^{106}Ru contaminant and examine how these align with the two plausible scenarios.

Reaction to form the homoleptic complex [Ru(ttpy)$_2$](PF$_6$)$_2$ (Fig. 1) was used as the reactive vehicle. Forceful reaction conditions by way of elevated temperature (154 °C), extended duration (16 h), and provision of dechlorinating agent (AgNO$_3$) were selected to encourage reaction completion (*Materials and Methods*). Interestingly, to date, such reactions have only been performed using Ru (III) (typically β-RuCl$_3$) or specially prepared Ru (II) halogenated compounds (47, 48). Only one literature reference was found pertaining to solvent reduction of a Ru (IV) compound, and this was carried out under microwave irradiation, unrelated to polypyridyl complexation (49). It is therefore quite interesting that this reaction system was found to be very effective for both Ru(III) and Ru(IV) precursors, to the extent that a potent oxidizing agent used in organic synthesis, KRuO$_4$ (50, 51), reacted appreciably while the highly refractory allotrope of RuCl$_3$, α-RuCl$_3$, was found to react smoothly and in essentially quantitative yield (Table 2). Such marked general reactivity using these conditions underscores the complete absence of reactivity observed in the case of RuO$_2$.

Radiochemical details are provided in *Materials and Methods*. For all reactions, we have coupled chromatography and radiography to demonstrate that ^{106}Ru has been incorporated into the isolated complex (i.e., [Ru(ttpy)$_2$](PF$_6$)$_2$ + [^{106}Ru(ttpy)$_2$](PF$_6$)$_2$). Here, we have used thin-layer chromatography (TLC) (normal phase, preparative scale) to demonstrate the purity of the isolated [Ru(ttpy)$_2$](PF$_6$)$_2$ by elution with an aqueous acetonitrile solution of high ionic strength. The decay progeny, ^{106}Rh [$t_{1/2}$ = 30 s, β$_{(mean)}$ = 1,410 keV] is a hard beta-particle emitter, making it well-suited to autoradiographic imaging. Prolonged exposure of the phosphor imaging plate (6 wk) yields darkened areas that

Table 2. Chemical yields of [Ru(ttpy)$_2$](PF$_6$)$_2$ and ttpyRuCl$_3$ from representative inorganic ruthenium compounds

Reactant	Ru ox. state	Solid-state form	[Ru(ttpy)$_2$](PF$_6$)$_2$, % yield	ttpyRuCl$_3$, % yield
Ru(NO)(NO$_3$)$_3$*	3$^+$	Molecular	92	No reaction[†]
(NH$_4$)$_2$RuCl$_6$	4$^+$	Molecular	96	No reaction
β-RuCl$_3$	3$^+$	Polymeric	94	88
α-RuCl$_3$	3$^+$	Polymeric	95	No reaction
KRuO$_4$	7$^+$	Molecular	19	No reaction
RuO$_2$	4$^+$	Polymeric	No reaction	No reaction

*Mixture in nitric acid. ox., oxidation.
[†]Reacted in presence of large excess of potassium chloride.

correlate to the $[Ru(ttpy)_2](PF_6)_2$ isolated from reactions involving ^{106}Ru-contaminated filter pieces and their aqueous extracts (*SI Appendix*, Fig. S22). As with all radiochemical experiments described herein, every effort to provide a full account of the initially measured ^{106}Ru activity has been made by measuring all subsequently isolated reaction products, by-products, and other relevant materials. In this way, the reactive and unreactive portions of the ^{106}Ru contaminant can be independently determined, where ^{106}Ru localized with $[Ru(ttpy)_2](PF_6)_2$ constitutes the reactive portion and ^{106}Ru measured in other materials and by-products (AgCl) constitutes the unreactive portion. For all reactions, a reasonably full account has been provided in consideration of the respective measurement uncertainty carried by each experimental component (General) and of the potential loss of material given the considerable number of mass transfer steps involved (*Radiochemistry*).

Direct Reaction with a Contaminated Filter Piece. Direct reaction of a portion (0.144 g, 7.99 ± 0.53 Bq) of the ^{106}Ru-contaminated filter piece in the presence of β-RuCl$_3$ resulted in 79.6 ± 4.9% (6.36 ± 0.39 Bq) of the ^{106}Ru being localized with the isolated $[Ru(ttpy)_2](PF_6)_2$ after gamma counting. The balance of the activity (unreactive portion) was reasonably well accounted for, with 8.62 ± 0.68% (0.689 ± 0.054 Bq) and 7.77 ± 0.60% (0.460 ± 0.035 Bq) measured in the remaining filter piece and the insoluble AgCl by-product, respectively.

Reactions Subsequent to Aqueous Extraction of a Filter Piece. To gain a bit more resolution, a similar reaction was performed on the aqueous extract of another filter piece. The ^{106}Ru that partitioned into the water extract (51.3 ± 2.4%, 6.14 ± 0.46 Bq) was found to be almost completely localized in the isolated $[Ru(ttpy)_2](PF_6)_2$ (95.3 ± 6.0%, 5.85 ± 0.37 Bq) with the balance of activity reasonably accounted for in the AgCl precipitate (6.06 ± 0.41%, 0.372 ± 0.025 Bq).

The filter piece was found to retain 27.8 ± 1.9% (3.33 ± 0.22 Bq) of the ^{106}Ru contaminant after aqueous extraction. The balance of ^{106}Ru activity (~20.9%) was most likely lost in transfer to the submicron filtration material which could not be accommodated in the well-detector space for measurement (*Gamma Spectrometry*). Direct reaction of the water-washed filter piece resulted in 75.2 ± 4.9% (2.50 ± 0.16 Bq) of the activity being localized in the isolated $[Ru(ttpy)_2](PF_6)_2$, with the balance reasonably accounted for in the AgCl by-product (16.2 ± 1.1%, 0.540 ± 0.038 Bq) and the remaining filter piece (9.06 ± 0.71%, 0.302 ± 0.024 Bq). Assuming that the activity remaining on the filter piece is representative of the entirety of ^{106}Ru that did not partition into the aqueous phase (i.e., 48.7 ± 2.4%) and summing reactive and unreactive contributions, we find that 85.6 ± 8.1% and 15.2 ± 1.4% of the initial ^{106}Ru contaminant to be reactive and unreactive, respectively. These results are in reasonably good agreement with those obtained by direct reaction on a ^{106}Ru-contaminated filter piece. Clearly, one or more of the water-insoluble components is chemically inert to the reaction conditions employed. According to Table 2, chemical inertness and a high degree of water insolubility are certainly consistent with the occurrence of RuO$_2$. Against the previously mentioned compositional characteristics for both trapping and pyroprocessing scenarios, the delineation of a small Ru(III) polychlorinated component (1.17 ± 0.36%) and a substantial water-insoluble, reactively inert component (~20%) consistent with RuO$_2$ support an origin from the reductive trapping of RuO$_4$ in HCl. Such activity further explains the high radiopurity of radio-ruthenium observed in environmental samples (1), since volatilization of β-RuO$_4$ from waste streams stands alone as the means to provide optimal separation efficiency (14).

Concluding Remarks

We have revealed compositional markers for the ^{106}Ru contaminant that are uniquely consistent with nuclear waste reprocessing, namely the reductive trapping of RuO$_4$ in HCl. This finding aligns

with other empirical evidence pertaining to radiopurity and age estimation (i.e., time since removal from irradiation) for spent nuclear fuel obtained from measurement of the ^{103}Ru:^{106}Ru ratio (1). An age estimate of ~2 y is considerably less than the usual time (≥3 y) allotted before reprocessing under typical reactor operating conditions (52). Therefore, a RuO$_4$ trapping process in HCl would undoubtedly be exothermic, exacerbating an already energetic mixture that, in light of the high volatility and potential explosive decomposition of RuO$_4$ (15), gives credence to the occurrence of an abrupt, uncontrolled release (i.e., explosion). Such conditions would certainly aid in the volatilization and dispersion of otherwise nonvolatile ruthenium species. For a facility undertaking the purification of fission products from spent nuclear fuel for commercial gain, it is hard to ignore the potential profit afforded by obtaining ^{106}Ru in high-specific activity, considering its long-standing medical use in the development of brachytherapy plaques for the treatment of eye cancer (53, 54). For this application, it is commonly electrodeposited from solution onto silver, along with the addition of carrier RuCl$_3$ (54, 55). Since this requires a highly soluble form of ^{106}Ru, it makes sense to invoke a reductive technique that generates polychlorinated Ru(III/IV) species with a high degree of radiopurity and aqueous solubility, rather than the vast majority of passivation techniques that ultimately produce the highly insoluble RuO$_2$.

In closing, the detection of ^{106}Ru in aerosol filters across European surveillance networks in 2017 represents a limiting case for forensic investigation, considering the high radiopurity of the contaminant and the absence of detectable signatures or anomalies from colocated stable elements. However, as this work has demonstrated, new opportunities arise when the radioisotope pertains to an element capable of covalent bond formation. By subjecting the radioactive contaminant to iterative, well-characterized chemical transformations and determining its subsequent fate and distribution, we create an inferential process from which we can gain both generalized and highly specific information about the chemical form(s) of the radioactive contaminant. This work constitutes direct evidence for specific nuclear fuel reprocessing activity and, coupled with other measurements and atmospheric dispersion modeling, provides irrefutable proof as to the origin of the 2017 environmental release of ^{106}Ru. Moreover, this work serves, by example, as a potentially valuable addition to the established suite of nuclear forensic capabilities.

Materials and Methods

General. Particulate filters containing ^{106}Ru from the radiological monitoring networks of Germany (German Meterological Services Deutscher Wetterdienst) and Sweden (Swedish Defense Research Agency Totalförsvarets forskninginstitut) were graciously donated. Chemical experimentation was conducted on portions of a particulate filter sample obtained from Vienna, Austria, and was composed of polypropylene (air collection from 2017-09-28 to 2017-10-04 at a rate of 675 m^3/h).

Chromatographic supports consisting of alumina (neutral, type WN-6, super grade, flash chromatography), silica (high-purity grade, 220 to 440 mesh, flash chromatography), and preparative TLC plates (glass-backed, 2.0-mm SiO$_2$ layer) were purchased from Sigma-Aldrich, Ltd. Columns (C$_{18}$, XBridge: 3.5 μm, 250 × 4.6 mm and 5 μm, 250 × 10 mm) were purchased from Waters, Ltd. for analytical and preparative-scale HPLC separations, respectively. All aqueous and ethanolic extracts of contaminated filter pieces were filtered through conditioned syringe filters (0.1-μm pore size; Fisher Scientific) prior to gamma counting and subsequent reaction.

Solvents and reagents were used as received. These include *N,N*′-dimethylformamide (Fisher Chemical, ACS grade), acetonitrile (Fisher Chemical, ACS grade), methanol (Fisher Chemical, Optima grade), dichloromethane (Fisher Chemical, ACS grade), diethyl ether (Fisher Chemical, ACS grade), potassium nitrate (Sigma-Aldrich, ≥ 99%), silver nitrate (Sigma-Aldrich, ≥ 99%), ammonium hexafluorophosphate (Acros Organics, 99%), 2-acetyl pyridine (Sigma-Aldrich, 99%), *p*-tolualdehyde (Sigma-Aldrich, 97%), β-ruthenium chloride hydrate (Sigma-Aldrich, reagent plus), ammonium hexachlororuthenate (Strem Chemicals, 99%), ruthenium (III) nitrosyl nitrate solution (Sigma-Aldrich, 1.5% Ru in 6.8 wt % nitric acid), ruthenium (IV)

oxide (Sigma-Aldrich, 99.9%), potassium perruthenate (Sigma-Aldrich), α-ruthenium chloride (Merck), and tetrabutylammonium chloride (Sigma-Aldrich, 98%).

Experimental uncertainty was derived by combining contributions from counting statistics, counting efficiency, and mass transfer (if applicable) in quadrature.

Synthesis and Characterization.

Synthesis of 4'-p-tolyl-2,2'; 6',2"-terpyridine (ttpy). Synthesis of this ligand resembled previously reported procedures (35, 36); however, these procedures were found to yield unsatisfactory purity considering the application. In our hands, 2-acetylpyridine (7.83 g, 0.065 mol and KOH aqueous solution (5 mL, 15 wt %) were stirred briefly in methanol (60 mL) at room temperature (~5 min). *p*-tolualdehyde (3.56 g, 0.03 mol) and concentrated ammonium hydroxide (25 mL) were then added and the mixture heated to reflux with vigorous stirring for 48 h. After cooling, the reaction mixture was decanted into a large separatory funnel. To this was added 600 mL of water and 600 mL of dichloromethane. After agitation, the dichloromethane layer was removed, washed once more with 600 mL water, then separated and dried over sodium sulfate. The dichloromethane was removed by distillation and the remaining residue was recrystallized from 95:5 ethanol/water to yield 2.45 g of slightly impure material. High purity was achieved by flash chromatography using 688 g of alumina, previously deactivated by thorough mixing with water (5% by mass) and using toluene as the mobile phase. Yield = 1.91 g (20%); ^{1}H NMR (600 MHz, d_6-DMSO) δ ppm: 2.40 (s, 3H, H$_{tolyl}$), 7.40 (d, J = 8.0 Hz, 2H, H$_{tolyl\ 3,5}$), 7.53 (dd, J = 7.5 Hz, J = 5.0 Hz, 2H, H$_{5,5''}$), 7.83 (d, J =8.0 Hz, 2H, H$_{tolyl\ 2,6}$), 8.04 (t, J = 7.5 Hz, 2H, H$_{4,4''}$), 8.67 (d, J = 8.0 Hz, 2H, H$_{3,3''}$), 8.70 (s, 2H, H$_{3',5'}$), 8.76 (d, J = 5.0 Hz, 2H, H$_{6,6''}$). ESI(+)MS found (calcd) for $C_{22}H_{17}N_3H$: 324.1511 (324.1501).

Synthesis of ttpyRuCl₃. This compound was prepared according to literature procedure. Note that reactant concentration should be maintained ≥0.01 M to attain high yield. Note also that the ethanol extract from a filter piece contaminated with ^{106}Ru, after filtration through a submicron filter, would be used in place of ethanol alone, according to the following typical preparation. The ligand ttpy (0.0825 g, 2.55 × 10$^{−4}$ mol) and RuCl₃ hydrate (0.0607 g, 2.32 × 10$^{−4}$ mol) were combined in 20 mL of ethanol (95%) and heated to reflux with agitation for 2 h. After cooling, the insoluble solid was isolated by filtration over a glass filter frit then agitated 5 to 10 min in ethanol (40 mL) and filtered. The residue was then rinsed with an additional portion of ethanol (40 mL) and finally with diethyl ether (40 mL). The solid was dried under vacuum. Yield = 0.123 g (88%). ESI(+)MS found (cald) from DMF solution for $C_{44}H_{34}N_6RuCl_3Na$: 554.9445 (554.9416).

Synthesis of [Ru(ttpy)₂](PF₆)₂ from β-RuCl₃.

Procedure (A). This compound was prepared similarly to literature procedures. Typically, the ligand ttpy (0.111 g, 3.42 × 10$^{−4}$ mol, 2.1 equivalents), RuCl₃ hydrate (0.0426 g, 1.63 × 10$^{−4}$ mol), and AgNO₃ (4.89 × 10$^{−4}$ mol) were combined in *N,N'*-DMF (reagent grade, 50 mL) and heated to reflux for 16 h. The reaction mixture was then cooled to room temperature, and the AgCl by-product was removed by vacuum filtration over a glass filter frit. The filtrate was then distilled to dryness and the residue chromatographed on silica using an acetonitrile/saturated, aqueous potassium nitrate (7:1) mixture as mobile phase. The isolated compound was transferred to a separatory funnel, followed by addition of water, NH₄PF₆, and enough dichloromethane to render a phase separation. After washing, the aqueous layer was removed and discarded. This process was repeated twice more, after which the organic phase was collected and distilled to dryness. The residue was then redissolved in acetonitrile and precipitated from water. This precipitate was collected by vacuum filtration, redissolved in acetonitrile, and precipitated from diethyl ether. This final precipitate was collected by filtration and dried under vacuum. Yield = 0.160 g (94%); ^{1}H NMR (600 MHz, CD₃CN) δ ppm: 2.54 (s, 3H, H$_{tolyl}$), 7.18 (dd, J = 8.0 Hz, J = 6.0 Hz, 2H, H$_{5,5''}$), 7.42 (d, J = 6.0 Hz, 2H, H$_{6,6''}$), 7.58 (d, J = 8.0 Hz, 2H, H$_{tolyl\ 3,5}$), 7.94 (t, J = 8.0 Hz, 2H, H$_{4,4''}$), 8.11 (d, J = 8.0 Hz, 2H, H$_{tolyl\ 2,6}$), 8.64 (d, J = 8.0 Hz, 2H, H$_{3,3''}$), 8.99 (s, 2H, H$_{3',5'}$). ESI(+)MS found (calcd) for $C_{44}H_{34}N_6Ru$ (M^{2+}): 373.9200 (374.0962).

Procedure (B). Alternatively, the ligand ttpy (0.111 g, 3.42 × 10$^{−4}$ mol, 2.1 equivalents) and RuCl₃ hydrate (0.0426 g, 1.63 × 10$^{−4}$ mol) were combined in ethanol (95%, 50 mL) and heated to reflux for 16 h. Distillation of the ethanol, followed by chromatographic isolation and work-up as outlined above in *Procedure (A)* gave the target complex in 89% yield (0.151 g). Notably, the same molar quantities and conditions applied to (NH₄)₂RuCl₆ and Ru(NO)(NO₃)₃ gave comparable yields (94 and 90%, respectively) for the formation of [Ru(ttpy)₂](PF₆)₂.

Synthesis of [Ru(ttpy)₂](PF₆)₂ from α-RuCl₃, (NH₄)₂RuCl₆, Ru(NO₃)₃(NO), KRuO₄, and RuO₂ in N,N'-DMF. These compounds were reacted, and subsequently isolated, according to the scale and conditions outlined in *Procedure (A)* for β-RuCl₃.

Yield (α-RuCl₃) = 0.162 g (95%); yield ((NH₄)₂RuCl₆) = 0.163 g (96%); yield (Ru(NO₃)₃(NO)) = 0.156 g (92%); yield (KRuO₄) = 0.032 g (19%); yield (RuO₂) = no reaction.

Gamma Spectrometry. The gamma detection system used was a small anode germanium (SAGe) well detector (GSW275L; Mirion Technologies) outfitted with a cosmic veto (plastic scintillator) detector to reduce the background (CV System-LM; Mirion Technologies). The SAGe well detector has a diameter of 28.00 mm and a depth of 40.00 mm with an active volume for the germanium crystal of 65.50 mm (thickness) by 86.6 mm (diameter). The resolution of the detector (full width at half maximum) is 1.835 keV at 1,332.5 keV. The gamma acquisition software used was Genie 2000 v3.4.1 (Mirion Technologies), with the counting efficiencies of the samples in the well of the SAGe counted simulated using LabSOCS v4.4.1 (Mirion Technologies). The analysis software used in quantifying the activity of ^{106}Ru was a peak-fitting and peak identification program called UniSAMPO (v 2.67)-Shaman (v 1.2), developed by Baryon Oy of Finland. The HPGe well detector was calibrated for energy and shape resolution using a National Institute of Standards and Technology–traceable standard (SRS 112559; Eckert & Ziegler) prior to measurement. Data were collected from 0 to 2,800 keV for 16,384 channels. Samples were counted in 20-mL glass scintillation vials (61 × 28 mm, outer dimensions). Detector count times varied greatly depending on the amount of ^{106}Ru in the sample and ranged anywhere from several thousand to several million seconds, ideally until an acceptable counting uncertainty was attained (<10%). Analysis was based upon the 622-keV gamma emission (9.93% abundance) associated with the ^{106}Ru progeny, ^{106}Rh, while decay corrections were performed using $t_{1/2}$ = 371.8 d for ^{106}Ru. For the experiment incorporating ^{106}Ru into ttpyRuCl₃, the purified reaction components were gamma counted until the critical limit (L$_c$) was exceeded and the peak was automatically identified by the peak search algorithm of the analysis software (UniSAMPO-Shaman, Baryon Oy, Finland). For instance, detection count times ranging from 1 to 2 Ms corresponded to detection capabilities, as defined by the L$_c$ and detection limit (L$_d$) at 95% confidence, of L$_c$ = 3.7 mBq, L$_d$ = 7.5 mBq and L$_c$ = 2.9 mBq, L$_d$ = 5.9 mBq, respectively.

NMR and Mass Spectrometry. The ^{1}H NMR spectra were acquired on a Bruker AVANCE III 600 MHz spectrometer by the University of Ottawa NMR Facility. Chemical shifts are reported relative to Me₄Si as an internal reference. Mass spectra were obtained using a Micromass Q-TOF II Electrospray Ionization Mass Spectrometer by the John L. Holmes mass spectrometry facility at the University of Ottawa.

HPLC. HPLC was performed using a Dionex ICS-6000 instrument equipped with photodiode array detector (PDA-1; Thermo Scientific), autosampler (AS-AP; Thermo Scientific), and fraction collector (ASX-280-FC; Thermo Scientific) and employing a C$_{18}$ column (3.5 μm, 250 × 4.6 mm and 5 μm, 250 × 10 mm) from Waters, Ltd. Chromeleon 7 (Thermo Scientific) was the software package used for instrument control and analysis. All injections and subsequent runs were monitored at both 254- and 450-nm wavelength.

Radiochemistry. Transformation of β-RuCl₃ to form either ttpyRuCl₃ or [Ru(ttpy)₂](PF₆)₂ in the presence of ^{106}Ru adhered to the respective protocols outlined above in *Synthesis and Characterization*. Typically, a filter piece was shaved with a razor into many thin pieces, and these were placed inside a scintillation vial for gamma counting prior to reaction. Once transferred to the reaction vessel, the empty scintillation vial was gamma-counted once more to ensure the efficacy of transfer.

Reactions with β-RuCl₃. For reaction to form ttpyRuCl₃ (*SI Appendix*, Fig. S16), the shaved filter pieces (1.03 ± 0.08 Bq ^{106}Ru) were immersed in 5 mL of ethanol and agitated in an ultrasound bath for 10 to 20 min, after which the ethanol was removed via syringe and filtered. The process was repeated twice more, and the ethanol fractions were combined and gamma-counted (0.074 ± 0.005 Bq ^{106}Ru). The ethanol washings were then transferred to a reaction vessel, along with an additional 5 mL of ethanol (rinse). The reaction protocol described herein for ttpyRuCl₃ (*Synthesis and Characterization*) was carried out, giving the target complex in 88% yield. This material was then gamma-counted, as were the subsequent components from its HPLC purification.

For direct reaction of a filter piece to form [Ru(ttpy)₂](PF₆)₂ (*SI Appendix*, Fig. S17), the gamma-counted filter shavings (7.99 ± 0.53 Bq ^{106}Ru) were transferred to a reaction vessel followed by the addition of 10 mL of water. After brief agitation in an ultrasound bath, the reaction protocol outlined herein for [Ru(ttpy)₂](PF₆)₂ was carried out (*Synthesis and Characterization*), giving a comparable yield for the final product (93%). All components

(i.e., [Ru(ttpy)$_2$](PF$_6$)$_2$, AgCl by-product, and the remaining filter pieces) were subsequently gamma-counted.

For reaction to form [Ru(ttpy)$_2$](PF$_6$)$_2$ from the aqueous extract (*SI Appendix*, Fig. S17), the shaved filter pieces (11.97 ± 0.89 Bq ^{106}Ru) were immersed in 5 mL of water and agitated for 10 to 20 min in an ultrasound bath, after which the water was separated via syringe and filtered. The process was repeated twice more, and the aqueous fractions were combined and gamma-counted. The aqueous extract was then transferred to a reaction vessel, followed by an additional 5 mL of water (rinse). Complexation was carried out according to the procedure described herein for [Ru(ttpy)$_2$](PF$_6$)$_2$ (*Synthesis and Characterization*), with the exception that a higher-proportion of DMF was used (60 mL). The target complex, [Ru(ttpy)$_2$](PF$_6$)$_2$, was isolated in 95% yield. All components (i.e., [Ru(ttpy)$_2$](PF$_6$)$_2$, AgCl by-product, and the remaining filter pieces) were subsequently gamma-counted. The remaining, washed filter pieces were reacted separately in DMF to give the isolated [Ru(ttpy)$_2$](PF$_6$)$_2$ in 94% yield, which was then gamma-counted along with the other reaction components.

Carrier-free reaction. Shaved filter pieces (0.48 ± 0.03 Bq ^{106}Ru) were immersed in 5 mL of ethanol and agitated in an ultrasound bath for 10 to 20 min, after which the ethanol was removed via syringe and filtered. The process was repeated twice more, and the ethanol fractions were combined and gamma-counted. The ethanol washings were concentrated by vacuum distillation then transferred with rinse solutions to a 3-mL conical reaction vessel. The ligand (0.20 mg, 6.18 × 10^{-7} mol) was added from a stock solution in ethanol to give a final reaction volume of 0.5 mL. A stir bar was added and a Teflon screw cap was secured. The reaction solution was agitated while immersed in an oil bath set to 90 °C for 16 h (*SI Appendix*, Fig. S18). After cooling to room temperature, the stir bar was removed and the reaction solution transferred to a distillation flask, followed by 20 mg of [Ru(ttpy)$_2$](PF$_6$)$_2$ (stable Ru). The solvent was removed by distillation, and the mixture was chromatographed on silica gel and worked up as previously described above in *Synthesis and Characterization*. The isolated complex was quantitatively recovered and gamma-counted.

Autoradiography. Autoradiography of chromatographed reaction products (*SI Appendix*, Figs. S21 and S22), isolated in the presence of ^{106}Ru, was performed on a BAS-5000 Image Analysis System (Fujifilm). Imaging plates (BAS-SR2025; GE Healthcare) were developed in closed imaging cassettes (EXPSR CASS. 20 × 25 cm; GE Healthcare) and erased (zeroed) using an IP Eraser 3 (Fujufilm). Images were acquired using BASReader software (Fujifilm) and processed using Multi Gauge v.3.1 (Fujifilm).

Data Availability. All relevant data and protocols (synthetic and radiochemical) are provided in the paper and *SI Appendix*.

1. O. Masson *et al.*, Airborne concentrations and chemical considerations of radioactive ruthenium from an undeclared major nuclear release in 2017. *Proc. Natl. Acad. Sci. U.S.A.* **116**, 16750–16759 (2019).
2. H. Ramebäck *et al.*, Measurements of ^{106}Ru in Sweden during the autumn 2017: Gamma-ray spectrometric measurements of air filters, precipitation and soil samples, and in situ gamma-ray spectrometry measurement. *Appl. Radiat. Isot.* **140**, 179–184 (2018).
3. I. Penev, H. Angelov, T. Arsov, S. Georgiev, N. Uzunov, ^{106}Ru aerosol activity observation above Southeast Europe in october 2017. *Dokl. Bulg. Akad. Nauk.* **71**, 613–618 (2018).
4. D. Jakab *et al.*, Methods, results and dose consequences of ^{106}Ru detection in the environment in Budapest, Hungary. *J. Environ. Radioact.* **192**, 543–550 (2018).
5. O. Saunier, D. Didier, A. Mathieu, O. Masson, J. Dumont Le Brazidec, Atmospheric modeling and source reconstruction of radioactive ruthenium from an undeclared major release in 2017. *Proc. Natl. Acad. Sci. U.S.A.* **116**, 24991–25000 (2019).
6. P. Bossew *et al.*, An episode of Ru-106 in air over Europe, september-october 2017 - geographical distribution of inhalation dose over Europe. *J. Environ. Radioact.* **205–206**, 79–92 (2019).
7. J. H. Sørensen, Method for source localization proposed and applied to the October 2017 case of atmospheric dispersion of Ru-106. *J. Environ. Radioact.* **189**, 221–226 (2018).
8. V. Shershakov, R. Borodin, Some results of determining the source and reasons for the appearance of 106Ru in Russia in september – october 2017. *IOP Conf. Ser. Mater. Sci. Eng.* **487**, 012002 (2019).
9. V. Shershakov, R. Borodin, Y. S. Tsaturov, Assessment of possible location Ru-106 source in Russia in September–October 2017. *Russ. Meteorol. Hydrol.* **44**, 196–202 (2019).
10. T. Hopp, D. Zok, T. Kleine, G. Steinhauser, Non-natural ruthenium isotope ratios of the undeclared 2017 atmospheric release consistent with civilian nuclear activities. *Nat. Commun.*, 10.1038/s41467-020-16316-3.
11. D. Zok, J. H. Sterba, G. Steinhauser, Chemical and radioanalytical investigations of ^{106}Ru-containing air filters from Vienna in fall 2017: Searching for stable element anomalies. *J. Radioanal. Nucl. Chem.* **318**, 415–421 (2018).
12. F. A. Cotton, G. Wilkinson, C. A. Murillo, M. Bochmann, "Part 3: The chemistry of the transition elements" in *Advanced Inorganic Chemistry*, (Wiley-Interscience, ed. 6, 1999), pp. 877–1084.
13. J. A. Rard, Chemistry and thermodynamics of ruthenium and some of its inorganic compounds and aqueous species. *Chem. Rev.* **85**, 1–39 (1985).
14. I. Kajan, ""Transport and containment chemistry of ruthenium under severe accident conditions in a nuclear power plant," doctoral thesis" (Chalmers University of Technology, Gothenburg, Sweden, 2016).
15. C. Mun, L. Cantrel, C. Madic, A literature review on ruthenium behaviour in nuclear power plant severe accidents. (2007). https://hal-irsn.archives-ouvertes.fr/irsn-00177621. Accessed 10 April 2018.
16. C. Lefebvre, T. Dumas, M.-C. Charbonnel, P. L. Solari, Speciation of ruthenium in organic TBP/TPH organic phases: A study about acidity of nitric solutions. *Procedia Chem.* **21**, 54–60 (2016).
17. P. Swain, C. Mallika, R. Srinivasan, U. Kamachi Mudali, R. Natarajan, Separation and recovery of ruthenium: A review. *J. Radioanal. Nucl. Chem.* **298**, 781–796 (2013).
18. K. Motojima, Removal of ruthenium from PUREX process. *J. Nucl. Sci. Technol.* **26**, 358–364 (1989).
19. I. Kajan, T. Kärkelä, A. Auvinen, C. Ekberg, Effect of nitrogen compounds on transport of ruthenium through the RCS. *J. Radioanal. Nucl. Chem.* **311**, 2097–2109 (2017).
20. N. Yoshida, T. Ohno, Y. Amano, H. Abe, Migration behaviour of gaseous ruthenium tetroxide under boiling and drying accident condition in a reprocessing plant. *J. Nucl. Sci. Technol.* **55**, 599–604 (2018).
21. M. A. El-Absy, M. A. El-Amir, M. Mostafa, A. A. Abdel Fattah, H. M. Aly, Separation of fission produced ^{106}Ru and ^{137}Cs from aged uranium targets by sequential distillation and precipitation in nitrate media. *J. Radioanal. Nucl. Chem.* **266**, 295–305 (2005).
22. N. L. Sonar *et al.*, Use of nickel sulfide-PMMA composite beads for removal of ^{106}Ru from alkaline radioactive liquid waste. *Sep. Sci. Technol.* **44**, 3753–3769 (2009).
23. S. Sato, N. Endo, K. Fukuda, Y. J. Morita, Optimization for removal of ruthenium from nitric acid solution by volatilizing with electrochemical oxidation. *Nucl. Sci. Tech.* **49**, 182–188 (2012).
24. P. Swain *et al.*, Separation and recovery of ruthenium from nitric acid medium by electro-oxidation. *J. Radioanal. Nucl. Chem.* **303**, 1865–1875 (2015).
25. J. M. Richards, B. J. Mincher, Selective partitioning of ruthenium from nitric acid media. *Solvent Extr. Ion Exch.* **35**, 49–60 (2017).
26. P. Kumar Verma, R. Bhikaji Gujar, P. Kumar Mohapatra, An efficient method for radio-ruthenium separation from acidic feeds: Extraction, transport and spectroscopic studies. *J. Environ. Chem. Eng.* **6**, 5830–5836 (2018).
27. F. Mousset, F. Bedioui, C. Eysseric, Electroassisted elimination of ruthenium from dissolved RuO$_2$xH$_2$O in nitric acid by using Ag(II) redox mediator: Toward a new insight into nuclear fuel reprocessing. *Electrochem. Commun.* **6**, 351–356 (2004).
28. P. Swain *et al.*, Separation of ruthenium from simulated nuclear waste in nitric acid medium using n-paraffin hydrocarbon. *Sep. Sci. Technol.* **49**, 112–120 (2014).
29. H. Meyer *et al.*, "Processes and devices for removing ruthenium as RuO$_4$ from ruthenate-containing solutions by distillation." US Patent Application Pub. US20120058043A1 (2012).
30. M. Balcerzak, E. Swicicka, Determination of ruthenium and osmium in each other's presence in chloride solutions by direct and third-order derivative spectrophotometry. *Talanta* **43**, 471–478 (1996).
31. M. Balcerzak, Analytical methods for the determination of ruthenium: The state of the art. *Crit. Rev. Anal. Chem.* **32**, 181–226 (2002).
32. G. L. Zimmerman, S. J. Riviello, T. A. Glauser, J. G. Kay, Photochemical decomposition of RuO$_4$. *J. Phys. Chem.* **94**, 2399–2404 (1990).
33. J. P. Sauvage, J. P. Collin, J. C. Chambron, S. Guillerez, C. Coudret, Ruthenium (II) and osmium (II) bis(terpyridine) complexes in covalently-linked multicomponent systems: Synthesis, electrochemical behaviour, absorption spectra, and photochemical and photophysical properties. *Chem. Rev.* **94**, 993–1019 (1994).
34. D. W. Thompson, I. Akitaka, T. J. Meyer, [Ru(bpy)$_3$]$^{2+*}$ and other remarkable metal-to-ligand charge transfer (MLCT) excited states. *Pure Appl. Chem.* **85**, 1257–1305 (2013).
35. J. Wang, G. S. Hanan, A facile route to sterically hindered and non-hindered 4′-Aryl-2,2′′:6′,2′′-terpyridines. *Synlett* **8**, 1251–1254 (2005).
36. K. Ohr, R. L. McLaughlin, M. E. Williams, Redox behavior of phenyl-terpyridine-substituted artificial oligopeptides cross-linked by Co and Fe. *Inorg. Chem.* **46**, 965–974 (2007).
37. B. P. Sullivan, J. M. Calvert, T. J. Meyer, Cis-trans isomerism in (trpy)(PPh$_3$)RuCl$_2$: Comparisons between the chemical and physical properties of a cis-trans isomeric pair. *Inorg. Chem.* **19**, 1404–1407 (1980).
38. J.-P. Collin *et al.*, Photoinduced processes in dyads and triads containing a ruthenium(II)-bis(terpyridine) photosensitizer covalently linked to electron donor and acceptor groups. *Inorg. Chem.* **30**, 4230–4238 (1991).
39. M. Rupp *et al.*, Photocatalytic hydrogen evolution driven by a heteroleptic ruthenium(II) bis-(terpyridine) complex. *Inorg. Chem.* **58**, 9127–9134 (2019).

40. P. A. Benavides, T. A. Matias, K. Araki, Unexpected lability of the [Ru^{III}(phtpy)Cl$_3$] complex. *Dalton Trans.* **46**, 15567–15572 (2017).

41. M. M. Taqui Khan, G. Ramachandraiah, R. S. Shukla, Ruthenium (III) chloride in aqueous solution: Kinetics of the aquation and anation reactions of the chloro complexes. *Inorg. Chem.* **27**, 3274–3278 (1988).

42. T. Suzuki *et al.*, Speciation of ruthenium (III) chloro complexes in hydrochloric acid solutions and their extraction characteristics with an amide-containing amine compound. *Metals* **8**, 558–568 (2018).

43. F. Mousset, C. Eysseric, F. Bediour, "Studies of dissolution solutions of ruthenium metal, oxide and mixed compounds in nitric acid." https://inis.iaea.org/collection/NCLCollectionStore/_Public/36/013/36013944.pdf?r=1. Accessed 5 December 2019.

44. A. A. Osipenko, V. A. Volkovich, Study of ruthenium behavior in alkali chloride melts using electronic absorption spectroscopy. *AIP Conf. Proc.* **2174**, 20045 (2019).

45. A. Merwin, M. A. Williamson, J. L. Willit, D. Chidambaram, Review – metallic lithium and the reduction of actinide oxides. *J. Electrochem. Soc.* **164**, H5236–H5246 (2017).

46. E.-Y. Choi, S. M. Jeong, Electrochemical processing of spent nuclear fuels: An overview of oxide reduction in pyroprocessing technology. *Pro. Nat. Sci. Mater.* **25**, 572–582 (2015).

47. R. Ziessel, V. Grosshenny, M. Hissler, C. Stroh, cis-[Ru(2,2′:6′,2′′-terpyridine)(DMSO) Cl(2)]: Useful precursor for the synthesis of heteroleptic terpyridine complexes under mild conditions. *Inorg. Chem.* **43**, 4262–4271 (2004).

48. I. P. Evans, A. Spencer, G. Wilkinson, Dichlorotetrakis (dimethyl sulphoxide) ruthenium(II) and its use as a source material for some new ruthenium (II) complexes. *J. Chem. Soc. Dalton Trans.* **2**, 204–209 (1973).

49. A. V. Bashilov, A. A. Fedorova, V. K. Runov, Reduction of ruthenium (IV) to ruthenium (III) in aqueous alcohol solutions of hydrochloric acid under microwave radiation. Ж. анал. химии **55**, 1250–1255 (2000).

50. R. Ciriminna *et al.*, Aerobic oxidation of alcohols in carbon dioxide with silica-supported ionic liquids doped with perruthenate. *Chemistry* **12**, 5220–5224 (2006).

51. A. J. Bailey, W. P. Griffith, S. I. Mostafa, P. A. Sherwood, Studies on transition-metal oxo and nitrido complexes: Perruthenate and ruthenate anions as catalytic organic oxidants. *Inorg. Chem.* **32**, 268–271 (1993).

52. A. S. Gerasimov, V. N. Kornoukhov, I. S. Sal'dikov, G. V. Tikhomirov, Production of high specific activity ^{144}Ce for artificial sources of antineutrinos. *At. Energy* **116**, 54–59 (2014).

53. B. Damato, I. Patel, I. R. Campbell, H. M. Mayles, R. D. Errington, Local tumor control after 106Ru brachytherapy of choroidal melanoma. *Int. J. Radiat. Oncol. Biol. Phys.* **63**, 385–391 (2005).

54. M. Hermida-López, L. Brualla, Technical note: Monte Carlo study of ^{106}Ru/^{106}Rh ophthalmic plaques including the ^{106}Rh gamma spectrum. *Med. Phys.* **44**, 2581–2585 (2017).

55. R. B. Manolkar *et al.*, The treatment of eye cancer. *Bhabha Atomic Research Centre Newsletter* **309**, 397–403 (2009).

CHEMISTRY